

Importance of the Second Binding Loop and the C-Terminal End of Cystatin B (Stefin B) for Inhibition of Cysteine Proteinases[†]

Ewa Pol and Ingemar Björk*

Department of Veterinary Medical Chemistry, Swedish University of Agricultural Sciences, Uppsala Biomedical Center, Box 575, SE-751 23 Uppsala, Sweden

Received March 2, 1999; Revised Manuscript Received May 25, 1999

ABSTRACT: The importance of residues in the second hairpin loop and the C-terminal end of mammalian cystatin B for binding of proteinases was elucidated by mutagenesis of the bovine inhibitor. Bovine cystatin B was modeled onto the crystal structure of the human inhibitor in complex with papain with minimal structural changes. Substitution of the two deduced contact residues in the second hairpin loop, Leu-73 and His-75, with Gly resulted in appreciably reduced affinities for papain and cathepsins H and B. These losses indicated that the two residues together contribute 20–30% of the free energy of binding of cystatin B to these enzymes and that Leu-73 is responsible for most of this contribution. In contrast, the small decrease in the affinity for cathepsin L suggested that the second hairpin loop is less important for inhibition of this proteinase. Replacement of the contact residue in the C-terminal end, Tyr-97, with Ala resulted in losses in affinity for papain and cathepsins L and H that were consistent with Tyr-97 contributing 6–12% of the energy of binding of cystatin B to these enzymes. However, this substitution minimally affected the affinity for cathepsin B, indicating that the C-terminal end is of limited importance for binding of this proteinase. All affinity decreases were due predominantly to increased dissociation rate constants. These results show that both the second hairpin loop and the C-terminal end of cystatin B contribute to anchoring the inhibitor to target proteinases, each of the two regions interacting with a different domain of the enzyme. However, the relative contributions of these two interactions vary with the proteinase.

Mammalian cystatin B (stefin B) is a reversible, competitive, and tight-binding protein inhibitor of papain-like cysteine proteinases (1–4). It is a member of family 1 (also called stefins) of the cystatin superfamily, which is divided into three families on the basis of sequence homology (1–4). The inhibitors of family 1 are primarily intracellular proteins, consisting of a single, ~100-amino acid chain that lacks disulfide bonds and carbohydrates. This family also contains mammalian cystatin A, bovine stefin C, and pig stefin D. The cystatins of family 2 are predominantly extracellular, consist of ~115 amino acids, have two disulfide bonds, and may be glycosylated. Members of this family are the mammalian inhibitors, cystatins C, S, and D, and chicken cystatin. The family 3 cystatins are the kininogens, which are glycosylated plasma proteins containing three copies of family 2-like cystatin domains, two of which can inhibit proteinases.

The physiological target enzymes of the mammalian cystatins are the lysosomal cysteine proteinases, primarily cathepsins B, H, K, L, and S (reviewed in ref 4). These proteinases, which are members of the papain superfamily,

are mainly involved in nonselective intracellular degradation of endogenous or exogenous proteins, but appear also to participate in specific processing of certain proteins via highly selective cleavages (5). The major role of the cystatins is presumably to protect cells and tissues from inappropriate proteolysis by these enzymes (4, 5). Cystatins also inactivate cysteine proteinases from parasites, e.g., cruzipain from *Trypanosoma cruzi* (6), and viruses (7, 8) and may participate in the defense against invasion of such infectious agents. In addition, they inhibit several plant cysteine proteinases, such as papain, which is frequently used as a model enzyme in structure–function studies.

Cystatin B has been isolated from human (9, 10), bovine (11), sheep (12), porcine (13), and rat (14) origins. It was found to be rather uniformly distributed among cells and tissues, consistent with a general protective role. However, evidence for more specific physiological functions of this inhibitor has also appeared. In humans, deficiency of cystatin B caused by mutations of the gene thus leads to a form of myoclonus epilepsy (15), and deletion of the gene in mice results in similar symptoms that appear to be caused by cerebellar apoptosis (16). Moreover, the correlation demonstrated between the concentrations of cystatins A and B in tumor tissue and malignant progression (17, 18) has led to the hypothesis that these cystatins may act as tumor suppressors.

The nature of the inhibition of cysteine proteinases by cystatins has been elucidated by determination of the three-dimensional structure of the complex of human cystatin B

[†] This work was supported by Swedish Council for Forestry and Agricultural Research Grant 32.0433/94 and Swedish Medical Research Council Grant 4212.

* To whom correspondence should be addressed: Department of Veterinary Medical Chemistry, Swedish University of Agricultural Sciences, Uppsala Biomedical Center, Box 575, SE-751 23 Uppsala, Sweden. Telephone: +46 18-4714191. Fax: +46 18-550762. E-mail: Ingemar.Bjork@vmk.slu.se.

and papain (19). The interactions between the two proteins in the complex are dominated by hydrophobic contacts which, from the inhibitor side, are provided by a wedge-shaped edge of the protein. This wedge consists of the N-terminal region, a first hairpin loop in the middle of the polypeptide chain, and a second hairpin loop closer to the C-terminus, with the C-terminal end of the chain appearing to provide additional contacts. Computer docking studies based on the structures of chicken cystatin and papain (20) are consistent with the general features of this interaction mechanism being similar for all cystatins. The large number of contacts formed result in highly stable complexes, with a K_d^1 as low as $\sim 10^{-14}$ M (21, 22).

The importance of the first hairpin loop of cystatins for the inhibition of proteinases appears to be well established (23, 24). The role of the second hairpin loop has been investigated for family 2 cystatins by chemical modification, deletion mutagenesis, and substitution of the Trp residue of this loop (24–26). However, the importance of the structurally different second hairpin loop of the family 1 inhibitors for proteinase binding, and the contribution of individual residues of this loop to the binding energy, have not been elucidated. Moreover, an interaction between the C-terminal end of cystatin B and papain, apparently not occurring in complexes of family 2 cystatins with the enzyme (20), has been proposed (19), but studies with deletion mutagenesis have challenged this conclusion (27).

In this work, we have determined the cDNA sequence for bovine cystatin B and expressed the inhibitor in its fully active form in large amounts for detailed studies. Moreover, we have characterized the inhibitory properties of bovine cystatin B, which have been sparingly investigated (28, 29), to assess the role of cystatin B in the defense against cysteine proteinases in the bovine. We have then used this inhibitor as a model to elucidate the importance of residues in the second binding loop and the C-terminal end of mammalian cystatin B for the binding of cysteine proteinases by site-directed mutagenesis.

MATERIALS AND METHODS

Proteins. The purification and properties of papain (EC 3.4.22.2) and the production of *S*-(methylthio)papain have been reported elsewhere (30–32). Cathepsins B (EC 3.4.22.1) and H (EC 3.4.22.6), both from human liver, were purchased from Calbiochem (San Diego, CA), and human liver cathepsin H was also purchased from Fitzgerald Industries International (Concord, MA). Cathepsin B from bovine kidney and cathepsin L (EC 3.4.22.15) from sheep liver (33) were gifts from I. Štern (J. Stefan Institute, Ljubljana, Slovenia) and R. W. Mason (Alfred I. du Pont Institute, Wilmington, DE), respectively. Chicken cystatin was isolated from egg white (30).

¹ Abbreviations: app, subscript denoting an apparent equilibrium or rate constant determined in the presence of an enzyme substrate; E-64, [*N*-(*L*-3-*trans*-carboxyoxiran-2-carbonyl)-*L*-leucyl]amido-4-guanidobutane; C3S-cystatin B, cystatin B variant in which Cys-3 is replaced with Ser; L73G/C3S-, H75G/C3S-, and Y97A/C3S-cystatin B, C3S-cystatin B variants in which Leu-73 and His-75 are replaced with Gly and Tyr-97 is replaced with Ala; k_{ass} , bimolecular association rate constant; K_d , dissociation equilibrium constant; k_{diss} , dissociation rate constant; K_i , inhibition constant; k_{obs} , observed pseudo-first-order rate constant; RACE, rapid amplification of cDNA ends; SDS–PAGE, sodium dodecyl sulfate–polyacrylamide gel electrophoresis.

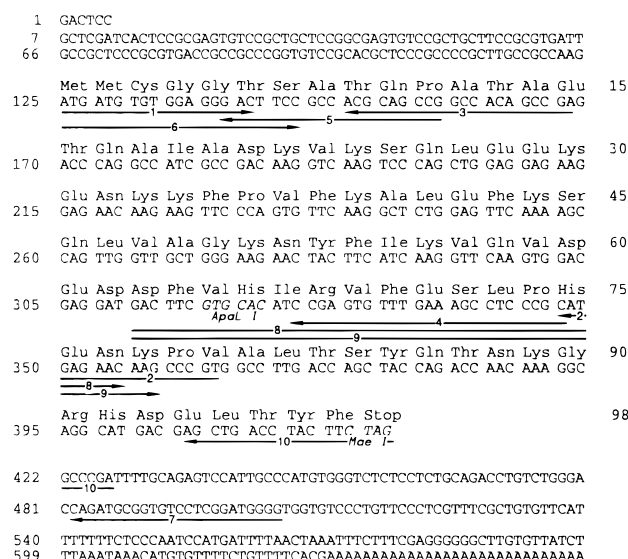


FIGURE 1: Amino acid sequence of bovine cystatin B and the nucleotide sequence obtained for the cDNA. The PCR primers used for the determination of the nucleotide sequence and for the generation of recombinant bovine cystatin B and mutants are denoted by arrows, numbered from 1 to 10, below the cDNA sequence. Most primers contained additional sequences that are not shown. Restriction sites used within the cystatin B cDNA are italic.

Determination of the cDNA Sequence of Bovine Cystatin B. Total RNA was isolated from calf liver within 2 h of the death of the animal with the CLONsep Total RNA Isolation Kit (Clontech Laboratories, Palo Alto, CA). Two degenerated PCR primers, denoted 1 and 2 (Figure 1), having appropriate restriction sites for insertion into the pUC 19 vector, were designed on the basis of the reported amino acid sequence of bovine cystatin B (11). With these primers, a cystatin B cDNA fragment was obtained by amplification of the mRNA population of the total RNA preparation with the Reverse Transcriptase RNA PCR Kit (Perkin-Elmer Cetus, Norwalk, CT) and with oligo(dT)₁₆ as a primer for the reverse transcription. This fragment was cloned into pUC 19 and sequenced.

From the DNA sequence obtained in this manner, new specific primers for the determination of the sequences of the 3'- and 5'-ends of the cDNA were constructed. With upstream primer 3 (Figure 1) and the downstream primer provided by the Marathon cDNA Amplification Kit (Clontech Laboratories), a 3'-RACE product, containing the remaining translated part of the cDNA and the 3'-untranslated region, was obtained from total RNA. The 5'-sequence was determined from bovine liver mRNA (Clontech Laboratories) with the 5'/3'-RACE kit (Boehringer Mannheim, Mannheim, Germany) in two successive steps with the downstream primers, 4 and 5 (Figure 1). The 3'- and 5'-fragments were cloned into a pCR II vector from the TA Cloning Kit (Invitrogen Corp., San Diego, CA) and sequenced. DNA sequencing was carried out with Sequenase version 2.0 (United States Biochemical, Cleveland, OH).

Expression of Cystatin B and Mutants. A vector designed previously for expression of cystatin A (34) was used also for expression of bovine cystatin B and mutants. This vector contains the sequence for the leader peptide for outer membrane protein A of *Escherichia coli*, which directs the expressed protein to the periplasmic space. This sequence

is followed by regions encoding a histidine tag and the recognition site for the endopeptidase, enterokinase, with which the histidine tag can be released (34, 35).

An insert for the expression of bovine cystatin B was constructed by PCR amplification of the cDNA region from nucleotide 125 to 503 with upstream primer 6 and downstream primer 7 (Figure 1). The template for this PCR was assembled from the cDNA fragment obtained with degenerated primers 1 and 2 and the 3'-RACE product (see above), which were both restricted with *Apa*LI (Figure 1) and ligated. Upstream primer 6 contained at its 5'-end 17 bases complementary to a region of the vector that included the codons for the enterokinase cleavage site and a *Taq*I site in the preceding segment encoding the linker to the histidine tag. In this primer, G in position 132 was replaced by C, which introduces a serine residue instead of a cysteine in position 3 of the protein. Downstream primer 7 included a *Bam*HI site at the 5'-end. The insert was cleaved with *Taq*I and *Bam*HI and ligated into the expression vector engineered to have the corresponding cohesive ends.

The C3S-cystatin B cDNA in the expression vector constructed as described above was used as a master gene for generation of the second-loop and C-terminal region variants by PCR. Upstream primers 8 for the L73G/C3S variant and 9 for the H75G/C3S variant (Figure 1) both contained the appropriate mismatches for the mutations and included an *Apa*LI site (Figure 1). For both mutations, downstream primer 7 (Figure 1) was that used for generation of the C3S-cystatin B cDNA (see above). The Y97A/C3S variant was produced with upstream primer 6 described previously (Figure 1) and downstream primer 10, which included the mismatch for the mutation and a *Mae*I site (Figure 1). The resulting PCR products, restricted with *Apa*LI and *Bam*HI or with *Taq*I and *Mae*I, were ligated into the C3S-cystatin B expression vector, from which the corresponding wild-type sequences had been excised with the same enzymes. Competent *E. coli* strain MC 1061 was transformed with the constructs for C3S-cystatin B and the mutants, and individual clones were collected and sequenced.

C3S-cystatin B and the three variants were expressed essentially as in previous work (34, 35), although expression was induced at 37 °C rather than at 42 °C to optimize the yield. The content of the periplasmic space was extracted by cold osmotic shock; the fusion proteins were isolated by affinity chromatography on a Ni²⁺ chelate column (Novagen, Inc., Madison, WI), and the free inhibitors were released by enterokinase cleavage (34, 35).

Spectroscopy. Far-ultraviolet (200–250 nm) circular dichroism spectra were recorded at room temperature in a Jasco J-41 A spectropolarimeter (Japan Spectroscopic Co., Tokyo, Japan) in cells with 0.1 cm path lengths and at protein concentrations of 0.2 g/L. The buffer was 0.05 M Tris-HCl (pH 7.4) containing 0.1 M NaCl and 0.1 mM EDTA. A mean-residue weight of 113, computed from the amino acid sequences, was used for all cystatin B forms in the calculation of mean-residue ellipticities.

Fluorescence emission spectra of papain, cystatin B forms, and the complexes of papain and the inhibitors were recorded as described previously (22, 30). Fluorescence emission difference spectra between the complexes and the free proteins were calculated from separately measured spectra (30).

Binding Stoichiometry. Stoichiometries for the binding of the cystatin B forms to papain were determined by titrations of 1 μ M S-(methylthio)papain (31) with the inhibitors. The titrations were monitored by the changes in tryptophan fluorescence emission accompanying the interaction (22, 30).

Inhibition Constants. Inhibition constants for the interactions of L73G/C3S-cystatin B with papain and of C3S-cystatin B and the L73G/C3S, H75G/C3S, and Y97A/C3S mutants with cathepsins L, H, and B were obtained from the equilibrium rates of cleavage of a fluorogenic substrate by the enzyme at increasing concentrations of the inhibitor, as described in detail previously (26, 32, 34). The substrate was carbobenzoxy-L-phenylalanyl-L-arginine 4-methylcoumaryl-7-amide (Peptide Institute, Osaka, Japan) for papain and cathepsin L, L-arginine 4-methylcoumaryl-7-amide (Bachem, Bubendorf, Switzerland) for cathepsin H, and carbobenzoxy-L-arginyl-L-arginine 4-methylcoumaryl-7-amide (Peptide Institute) for cathepsin B. The substrate concentrations were 20 μ M for papain, 10 μ M for cathepsins L and B, and 50 μ M for cathepsin H; the extent of substrate hydrolysis never exceeded 5%. The inhibitor concentration was varied from 0.1–2 $K_{i, app}$ to 2–14 $K_{i, app}$ and was at least 10-fold higher than that of the enzyme. Values of $K_{i, app}$ were obtained by nonlinear regression analyses of plots of the ratio of the inhibited to uninhibited rates of substrate hydrolysis against inhibitor concentration (32) and were corrected for substrate competition to give K_i . Most K_m values used in these corrections have been reported elsewhere (34). The K_m of carbobenzoxy-L-arginyl-L-arginine 4-methylcoumaryl-7-amide for bovine cathepsin B under the conditions of the K_i measurements was determined to $26 \pm 5 \mu$ M.

Association Kinetics. The rates of binding of all cystatin B variants to papain and cathepsin L, of C3S-cystatin B and the H75G/C3S variant to cathepsin H, and of the Y97A/C3S variant to cathepsin B were evaluated under pseudo-first-order conditions by continuous measurements of the loss of enzyme activity in the presence of a fluorogenic substrate, essentially as in earlier work (26, 32, 34). The inhibitor concentrations were at least 10-fold higher than those of the enzymes and were varied from a lower limit of 0.2–1 nM to an upper limit of 5–10 nM for reactions with papain and cathepsins L and H, whereas the range was 2–10 μ M for reactions with cathepsin B. The substrates for the enzymes, their concentrations, and maximal levels of substrate hydrolysis were the same as in the measurements of K_i . Values of $k_{obs, app}$ were obtained by nonlinear least-squares regression analyses of the progress curves (32). $k_{ass, app}$ was computed from the slopes of plots of $k_{obs, app}$ versus inhibitor concentration and was corrected for substrate competition to give k_{ass} as described above.

Dissociation Kinetics. The rates of dissociation of the complexes of C3S-cystatin B or the H75G/C3S-cystatin B variant and papain were analyzed by virtually irreversibly trapping the enzyme dissociated from 10 μ M complex with 100–215 μ M chicken cystatin (form 2). Chicken cystatin binds considerably tighter to papain than cystatin B or its variants (21) and therefore prevents reassociation of the liberated cystatin B forms with the enzyme. The slow dissociation was monitored by the appearance of the tight complex of the displacing chicken cystatin and the released papain, which was analyzed by HPLC on a Mono Q column (Amersham Pharmacia Biotech, Uppsala, Sweden) as de-

scribed earlier (21, 22). The rate of dissociation of the complex of the Y97A/C3S variant and papain was similarly studied by reacting the enzyme dissociating from the complex (1 μ M) with 3–20 μ M chicken cystatin (form 1). The progress of this more rapid dissociation was monitored in a conventional fluorimeter by the decrease of tryptophan fluorescence accompanying formation of the chicken cystatin–papain complex, as in previous work (34). In both these analyses, the synthetic cysteine proteinase inhibitor, E-64, was added in a 2-fold molar ratio to papain immediately after the cystatin B variants and the enzyme were mixed to prevent proteolysis which might be caused by contaminating cysteine proteinases not inactivated by the protein inhibitors. Excess E-64 was then removed by gel chromatography before chicken cystatin was added (22).

The dissociation rate of the complex of L73G/C3S-cystatin B and cathepsin H was investigated by trapping cathepsin H released from 100 nM complex with 5 μ M C3S-cystatin B, which binds considerably tighter to the enzyme than the L73G/C3S variant (see the Results). The rate was monitored in an Applied Photophysics (Leatherhead, U.K.) SX-17MV stopped-flow fluorimeter by the accompanying decrease in tryptophan fluorescence. This decrease was caused by the complex of the displacing C3S-cystatin B with cathepsin H having a lower fluorescence than that of the L73G/C3S variant with the enzyme, which is analogous with the behavior of the corresponding complexes with papain (see the Results). In all analyses of dissociation kinetics, k_{diss} was obtained by nonlinear least-squares regression analysis of the exponential progress curves.

Miscellaneous Procedures. SDS–PAGE was performed on 16.5% (w/v) gels with the Tricine buffer system (34). N-Terminal sequences were determined as described in ref 21. Relative molecular masses of the cystatin B variants were determined by MALDI mass spectroscopy (34).

Modeling. The coordinates for the human cystatin B–papain complex (19) (PDB file name 1STF) were used to model the complex of bovine cystatin B and papain. Amino acids were replaced with the graphics program O (36), keeping the backbone unaltered as bovine and human cystatin B have the same number of residues and highly similar sequences, and the most favorable rotamer for each new side chain was chosen.

Experimental Conditions and Protein Concentrations. All analyses of inhibitor–proteinase binding were carried out at 25 ± 0.2 °C. The buffers that were used were as follows: for papain, 0.05 M Tris-HCl (pH 7.4) containing 0.1 M NaCl and 0.1 mM EDTA, and in all analyses except the measurements of dissociation rate constants 1 mM dithiothreitol and 0.01% (w/v) Brij 35; for cathepsin L, 0.1 M sodium acetate (pH 5.5) containing 1 mM EDTA, 1 mM dithiothreitol, and 0.01% (w/v) Brij 35; for cathepsin H, 0.1 M sodium phosphate (pH 6.8) containing 1 mM EDTA and 1 mM dithiothreitol; and for cathepsin B, 0.05 M Mes-NaOH (pH 6.0) containing 0.1 M NaCl, 0.1 mM EDTA, 1 mM dithiothreitol, and 0.1% (w/v) poly(ethylene glycol).

Concentrations of papain and bovine cathepsin B were determined by absorption measurements at 280 nm from molar absorption coefficients of 55 900 (30) and 61 400 $\text{M}^{-1} \text{cm}^{-1}$, calculated from the amino acid sequence (37, 38), respectively. The weight concentrations and relative molecular masses of human cathepsin B and of cathepsin H were

provided by the manufacturers. The molar concentration of cathepsin L was obtained by titration with E-64 (33). Concentrations of cystatin B forms were determined by absorption measurements at 280 nm from molar absorption coefficients, calculated from the amino acid sequences (38), of 4470 $\text{M}^{-1} \text{cm}^{-1}$ for C3S-, L73G/C3S-, and H75G/C3S-cystatin B and 2980 $\text{M}^{-1} \text{cm}^{-1}$ for Y97A/C3S-cystatin B.

RESULTS

Determination of the cDNA Sequence for Bovine Cystatin B. The aim of this work required that the bovine cystatin B cDNA sequence be determined to allow production of a recombinant inhibitor and mutants thereof. In the first step of this analysis, PCR with cDNA synthesized from the mRNA population of a preparation of bovine liver total RNA as a template and with degenerated primers gave a cDNA fragment comprising base pairs 125–363 (Figure 1). 3'-RACE with a specific upstream primer gave a further sequence of 480 bp (base pairs 149–628; Figure 1), establishing the remaining 58 bp of the cystatin B coding region as well as the entire 3'-untranslated region. With purified bovine liver mRNA as a template and two specific downstream primers, 124 nucleotides of the 5'-untranslated region were obtained by 5'-RACE, which together with the sequences determined previously gave a 628 bp bovine cystatin B cDNA (Figure 1). Alignment with the cDNA of human cystatin B (15) showed that 81% identity existed between the coding regions, whereas the noncoding regions exhibited no significant similarity.

Modeling. Both bovine and human cystatin B have 98 amino acids, 76 of which are identical (10, 11). This high degree of similarity allowed modeling of bovine cystatin B onto the polypeptide chain backbone of human cystatin B in complex with papain (19). This modeling showed that all 22 side chains that were different in the bovine inhibitor could be well accommodated in the structure of the human inhibitor, with minimal changes of the contacts with the proteinase. In particular, the structures of and contacts made by the N-terminal region, the second hairpin loop, and the C-terminal end were unaltered, as the two cystatin B forms have the same sequence in these regions. The only observable difference in the binding surface was in the first hairpin loop, in which a Val to Leu replacement in the conserved Gln-Val-Val-Ala-Gly sequence caused a minor change in the enzyme contact. The crystal structure of the complex and these modeling studies suggested that, of the residues in the second binding loop and the C-terminal end, Leu-73 and His-75 in the former and Tyr-97 in the latter are primarily involved in the interactions with papain (19). These residues were mutated to Gly or Ala to probe their contribution to the inhibition of target proteinases.

Expression and General Properties of Cystatin B and Mutants. Bovine cystatin B and the L73G, H75G, and Y97A mutants were all expressed as variants with a Cys-3 to Ser substitution because of the reported possibility of wild-type cystatin B forming inactive, disulfide-linked dimers (39). The final yields of the four forms after purification varied from 9 to 14 mg/L of bacterial culture. The purified inhibitors all exhibited one band with an apparent molecular mass of ~11000 Da as determined by SDS–PAGE under reducing conditions, indicating >99% purity.

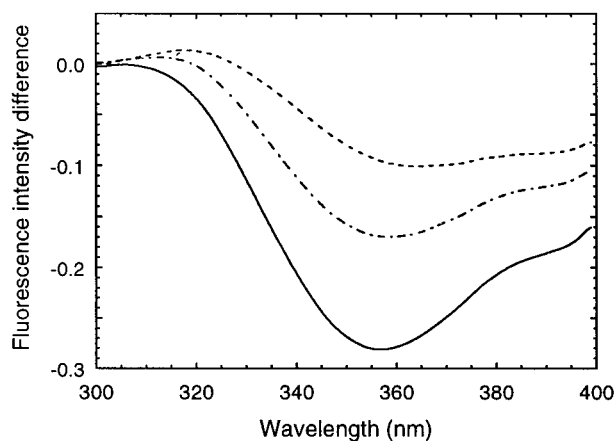


FIGURE 2: Fluorescence emission difference spectra between complexes of bovine cystatin B or second-loop mutants with papain and the free proteins: (—) C3S-cystatin B, (---) L73G/C3S-cystatin B, and (-·-·-) H75G/C3S-cystatin B. The papain concentration was 1 μ M, and the molar ratio of inhibitors to papain was 1.2, giving >99% saturation of the enzyme. Before calculation of the difference spectra, all measured spectra were normalized to a fluorescence intensity of 1.0 for free papain at the wavelength of the emission maximum.

N-Terminal sequence analyses of C3S-cystatin B gave the expected sequence, verifying the desired amino acid substitution as well as correct cleavage by enterokinase. The molecular masses, determined by MALDI mass spectroscopy, of both C3S-cystatin B and the three mutants were within 3 mass units (0.03%) of the expected values. The far-ultraviolet circular dichroism spectra of C3S-cystatin B and the three mutants all had broad minima at about 218 nm with identical mean-residue ellipticities of $5000 \pm 200 \text{ deg cm}^2 \text{ dmol}^{-1}$ (not shown) and were comparable with that of recombinant human cystatin B (40). Titrations, monitored by the decrease in tryptophan fluorescence accompanying the interaction (see below) (30, 31), of *S*-(methylthio)papain with the inhibitors gave binding stoichiometries of 1.00 ± 0.05 for all cystatin B variants.

Together, these results indicate that all four variants had the correct length and mass, were properly folded, and were fully active in proteinase binding. In particular, the molecular masses, together with the cDNA sequencing, show that the mutants had the intended amino acid replacements. Moreover, the circular dichroism spectra are consistent with the second-loop and C-terminal region mutations not having caused any conformational changes of the protein.

Fluorescence Changes on Interaction with Papain. The binding of C3S-cystatin B and the two second-loop mutants, L73G/C3S- and H75G/C3S-cystatin B, to papain was accompanied by shifts of the maxima of the fluorescence emission spectra to shorter wavelengths and reductions of fluorescence emission intensity, as reflected by difference spectra between the complexes and the free proteins (Figure 2). The fluorescence changes for C3S-cystatin B were comparable to those for human cystatin C (22) but substantially larger than those for human cystatin A (34). The binding of the two mutants to papain induced appreciably smaller changes than C3S-cystatin B, the difference being more pronounced for the L73G/C3S than for the H75G/C3S mutant.

Kinetics and Affinity of Interaction with Cysteine Proteinases. Equilibrium and rate constants were determined for the

binding of the cystatin B forms to papain and cathepsins L, H, and B (Table 1). The methods that were used depended on the affinity and kinetics of the interactions and the amount of enzyme available.

In most cases, K_d was determined as K_i , but was calculated from separately measured values of k_{ass} and k_{diss} for some tight interactions with papain (Table 1). The K_i values determined for the binding of C3S-cystatin B or the H75G/C3S mutant to cathepsin L and of the Y97A/C3S mutant to cathepsin B are somewhat uncertain. The reason is that the lowest inhibitor concentrations that could be studied were only about $2K_{i,\text{app}}$, instead of ideally below $K_{i,\text{app}}$, because of the instability of the enzymes at the long reaction times (>3 h) that were necessary for measurements at lower concentrations. Moreover, the low affinity of L73G/C3S-cystatin B for cathepsin B only allowed estimation of a lower limit for K_i .

The k_{ass} for most interactions could be measured by continuously monitoring the loss of enzyme activity in the presence of a fluorogenic substrate in a conventional fluorimeter (Table 1). In all these analyses, $k_{\text{obs,app}}$ exhibited a linear dependence on the inhibitor concentrations within the covered ranges. The observed rates of certain interactions with cathepsins H and B were too high to be monitored by this procedure, presumably due to a high k_{diss} , and the high enzyme concentrations required for stopped-flow fluorimetry precluded the use of this method. However, k_{ass} for the binding of L73G/C3S-cystatin B to cathepsin H could be calculated from K_d and k_{diss} (Table 1).

Values of k_{diss} for the interactions of C3S-cystatin B or the H75G/C3S and Y97A/C3S mutants with papain were measured by trapping the enzyme dissociating from the complexes with an excess of chicken cystatin (Table 1). The rates were monitored by the appearance of the new complex of the displacing chicken cystatin and papain, which was analyzed either by ion-exchange chromatography or by the resulting decrease of tryptophan fluorescence. k_{diss} for the interaction between L73G/C3S-cystatin B and cathepsin H was measured in a similar manner, but with C3S-cystatin B as the displacing inhibitor, and by analyses of the accompanying fluorescence decrease in a stopped-flow fluorimeter (Table 1). The low observed fluorescence change caused a substantial uncertainty in this value. In most cases, k_{diss} was not determined directly, mainly due to the lack of appropriate methods, but was calculated from K_d and k_{ass} (Table 1). Values of k_{diss} for the interactions of the L73G/C3S mutant with papain or cathepsin L were also estimated, with appreciable error, from the intercepts on the ordinate of the plots of the observed pseudo-first-order rate constants versus inhibitor concentration (Table 1) and were comparable to the calculated values.

DISCUSSION

In this work, bovine cystatin B and the second-loop and C-terminal region mutants were expressed as Cys-3 to Ser variants, as in previous studies of the X-ray structure of the human cystatin B–papain complex and of the proteinase-binding properties of the human inhibitor (19, 41). By this replacement, the formation of inactive, disulfide-linked dimers (39) during isolation and analyses was avoided. The affinity determined for the interaction of bovine C3S-cystatin

Table 1: K_d , k_{ass} , and k_{diss} for the Binding of Bovine Recombinant C3S-Cystatin B and the L73G/C3S, H75G/C3S, and Y97A/C3S Mutants to Cysteine Proteinases^a

enzyme	cystatin B form	K_d (M)	k_{ass} ($\text{M}^{-1} \text{s}^{-1}$)	k_{diss} (s^{-1})
papain	C3S	$1.2 \times 10^{-12} {}^b$ [1]	$(6.8 \pm 0.2) \times 10^6$ (8) [1]	$(8.0 \pm 0.2) \times 10^{-6}$ (3) [1]
	C3S/L73G	$(4.2 \pm 0.2) \times 10^{-10}$ (11) [350]	$(2.5 \pm 0.1) \times 10^6$ (10) [0.4]	$1.1 \times 10^{-3} {}^c$ [138] $(1.2 \pm 0.5) \times 10^{-3}$ (10) ^d
cathepsin L	C3S/H75G	$2 \times 10^{-11} {}^b$ [17]	$(2.4 \pm 0.1) \times 10^6$ (10) [0.4]	$(4.6 \pm 0.1) \times 10^{-5}$ (3) [6]
	C3S/Y97A	$5.6 \times 10^{-11} {}^b$ [48]	$(6.8 \pm 0.3) \times 10^6$ (9) [1]	$(3.8 \pm 0.3) \times 10^{-4}$ (7) [48]
	C3S	$(9.3 \pm 0.6) \times 10^{-12}$ (14) [1]	$(1.8 \pm 0.1) \times 10^7$ (16) [1]	$1.7 \times 10^{-4} {}^c$ [1]
	C3S/L73G	$(9.4 \pm 0.6) \times 10^{-11}$ (16) [10]	$(1.3 \pm 0.1) \times 10^7$ (14) [0.7]	$1.2 \times 10^{-3} {}^c$ [7] $(1.1 \pm 0.2) \times 10^{-3}$ (14) ^d
cathepsin H	C3S/H75G	$(9.2 \pm 0.5) \times 10^{-12}$ (12) [1]	$(1.7 \pm 0.1) \times 10^7$ (10) [1]	$1.6 \times 10^{-4} {}^c$ [1]
	C3S/Y97A	$(4.8 \pm 0.1) \times 10^{-11}$ (15) [5.2]	$(1.3 \pm 0.1) \times 10^7$ (11) [0.7]	$6.2 \times 10^{-4} {}^c$ [3.6]
	C3S	$(5.2 \pm 0.3) \times 10^{-10}$ (10) [1]	$(1.7 \pm 0.1) \times 10^6$ (10) [1]	$9 \times 10^{-4} {}^c$ [1]
	C3S/L73G	$(2.5 \pm 0.1) \times 10^{-8}$ (11) [48]	$2 \times 10^6 {}^e$ [1.2]	0.05 ± 0.02 (9) [56]
	C3S/H75G	$(1.2 \pm 0.1) \times 10^{-9}$ (11) [2.3]	$(1.3 \pm 0.1) \times 10^6$ (9) [0.8]	$1.6 \times 10^{-3} {}^c$ [1.8]
cathepsin B (human)	C3S/Y97A	$(4.1 \pm 0.2) \times 10^{-9}$ (10) [8]	ND ^f	ND
	C3S	$(6.7 \pm 0.4) \times 10^{-6}$ (7) [1]	ND	ND
	C3S/L73G	$\geq 1.4 \times 10^{-4}$ (2) [>21]	ND	ND
	C3S/H75G	$(1.3 \pm 0.1) \times 10^{-5}$ (8) [2]	ND	ND
cathepsin B (bovine)	C3S/Y97A	$(9 \pm 1) \times 10^{-6}$ (7) [1.3]	130 ± 3 (10)	$1.2 \times 10^{-4} {}^c$
	C3S	$(8.2 \pm 0.6) \times 10^{-6}$ (7) [1.2]	ND	ND

^a The methods and buffers used in the determinations are given in Materials and Methods. Measured values are reported as means \pm the standard error of the mean with the number of measurements in parentheses. Calculated values are given without errors. Relative values, defined as $K_{i,\text{mutant}}/K_{i,\text{C3S-cystatin B}}$, $k_{\text{ass,C3S-cystatin B}}/k_{\text{ass,mutant}}$, and $k_{\text{diss,mutant}}/k_{\text{diss,C3S-cystatin B}}$, are given in square brackets. Relative values >1 thus indicate changes of K_i , k_{ass} , and k_{diss} that are expected to result in a binding affinity that is lower than that of C3S-cystatin B. ^b Calculated from k_{ass} and k_{diss} . ^c Calculated from K_i and k_{ass} . ^d Obtained from the intercepts of plots of the observed pseudo-first-order rate constants vs inhibitor concentration. ^e Calculated from K_i and k_{diss} . ^f Not determined.

B with papain ($K_d \sim 10^{-12}$ M) is about 100-fold higher than that obtained previously for the wild-type bovine inhibitor (28). The difference is due to the much lower dissociation rate constant that was measured by a displacement procedure in our work, whereas the association rate constants are nearly identical in the two studies. This discrepancy is presumably caused primarily by difficulties in the earlier work in accurately measuring the very low dissociation rate constant by progress-curve analyses of the loss of enzyme activity. In contrast, the somewhat weaker binding of C3S-cystatin B to cathepsin L ($K_d \sim 10^{-11}$ M) is of comparable strength as that reported earlier for the wild-type inhibitor (28, 29), both the association and dissociation rate constants being similar. These findings indicate that the Cys-3 to Ser substitution has not adversely affected the binding of bovine cystatin B to target proteinases. This conclusion is supported by the three-dimensional structure of the human cystatin B–papain complex (19) and by mutagenesis of Cys-3 of human cystatin B (23).

As for other cystatins, the affinities of bovine cystatin B for the exopeptidases cathepsins H and B ($K_d \sim 5 \times 10^{-10}$ and 7×10^{-6} M, respectively), which have not been determined previously, are appreciably lower than those for papain or cathepsin L. The weaker binding is caused both by lower association rate constants and higher dissociation rate constants. This behavior is presumably due to the additional polypeptide chain segments that block the active site clefts of cathepsins H and B (42, 43).

Bovine cystatin B has a 10–100-fold higher affinity for papain than reported previously for cystatin B from humans, pigs, and sheep (9, 12, 13, 23, 41, 44), although problems in determining high affinities by equilibrium methods are likely also to be at least partly responsible for these differences. In contrast, the affinity of the bovine inhibitor for cathepsin L is comparable with those reported for the inhibitors from the other three species (9, 12, 13, 29, 41).

Bovine cystatin B may bind cathepsin H up to about 20-fold more weakly than the inhibitors from humans and pigs, the only species variants for which the binding to cathepsins H and B has been investigated, but this difference is uncertain, as the published values vary appreciably (9, 13, 23, 41, 45). However, it appears to be clear that the affinity of bovine cystatin B for cathepsin B, regardless whether of human or bovine origin, is substantially (about 100-fold) lower than those of the human and porcine inhibitors for this enzyme (9, 13, 23, 44, 45). This behavior is unexpected in view of the great similarity between bovine and human cystatin B suggested by the modeling studies. It is possible that the only observable structural difference in the binding surface, the Val to Leu substitution in the first hairpin loop, is the cause of the lower affinity, although this replacement would be expected to affect also the binding to papain and cathepsin L. A more likely possibility is structural changes close to the second hairpin loop, which is the region of the inhibitor expected to collide with the occluding loop that partially covers the active site of cathepsin B (42). Potentially responsible residues are Glu-71, which is Gln in human cystatin B (although it is Glu in the porcine inhibitor), and Val-80 and Ala-81, which are Leu and Thr, respectively, in human and porcine cystatin B. It is also possible that Gly-5 and Thr-6 in the N-terminal region, replacing Ala and Pro, respectively, present in all other known species variants of cystatin B, contribute to the weaker binding of cathepsin B. However, these substitutions would also be likely to affect the interactions with papain and cathepsin L. The origin of the reduced affinity of bovine cystatin B for cathepsin B has relevance for an understanding of the mechanism of inhibition of this enzyme by cystatins, which appears to differ from that of enzymes with easily accessible active sites (32, 42, 46).

Bovine cystatin B was used as a model to characterize the contribution of residues in the second hairpin loop and

the C-terminal region of mammalian cystatin B to the binding of cysteine proteinases. The high degree of sequence similarity between different forms of cystatin B (10–13, 47), together with the nearly identical structures of bovine and human cystatin B indicated by computer modeling and the comparable inhibition of most proteinases by different species variants, suggests that the results can be extended also to other such variants. Nevertheless, the general validity of the conclusions may be somewhat uncertain for cathepsin B inhibition because of the weaker binding of this proteinase by bovine cystatin B than by the other species variants for which data are available.

Substitution of either of the two inferred contact residues in the second binding loop of cystatin B, Leu-73 and His-75, with Gly led to a loss of the affinity of the inhibitor for all the proteinases that were studied. The decrease was larger in the case of the L73G variant and was ~350-fold, compared with the affinity of the parent inhibitor, for papain, ~10-fold for cathepsin L, ~50-fold for cathepsin H, and >20-fold for cathepsin B. In contrast, substitution of His-75 resulted in a decrease of only ~20-fold for papain and ~2-fold for cathepsins H and B and did not detectably affect the binding to cathepsin L. These results suggest that no single residue in the second hairpin loop of cystatin B is as important for the binding of cysteine proteinases as Trp-106 in this loop of the family 2 inhibitor, cystatin C. Substitution of this residue with Gly thus reduced proteinase affinities by 300–900-fold (26). However, Leu-73 and His-75 in cystatin B together contribute energies of binding to papain and cathepsin H comparable to that of Trp-106 in cystatin C (26). This joint contribution amounts to ca. –21 and ca. –12 kJ mol⁻¹, respectively, i.e., ~30 and ~20%, respectively, of the total unitary free energy of binding² (48) of the parent inhibitor to the two enzymes. Leu-73, which is conserved in all mammalian family 1 cystatins characterized so far (1, 2, 10–13, 47), is responsible for most of this binding energy. The combined contribution of the two residues to cathepsin B binding may be comparable with those to papain and cathepsin H binding, but the low affinity of the L73G variant precluded an assessment of this effect. In contrast, the joint contribution of Leu-73 and His-75 to cathepsin L binding is considerably smaller, amounting to only ~8 kJ mol⁻¹, i.e., <10% of the total binding energy of the control inhibitor. The second binding loop of cystatin B thus appears to be less important for binding of cathepsin L than for binding of the other enzymes.

Sequence alignment shows that family 1 cystatins have a C-terminal extension of nine residues, compared with cystatins from family 2 (19, 20, 49). This region in cystatin B was suggested to provide an additional interaction with cysteine proteinases (19). Mutation of the deduced contact residue, Tyr-97 (19), to Ala resulted in an affinity decrease of ~50-fold for papain, ~5-fold for cathepsin L, and ~8-fold for cathepsin H, whereas the binding of cathepsin B was not detectably affected. The contribution of Tyr-97 to binding of papain and cathepsins L and H is thus intermediate to those of Leu-73 and His-75 in the second binding loop, accounting for a binding energy of –4 to –9 kJ mol⁻¹, i.e.,

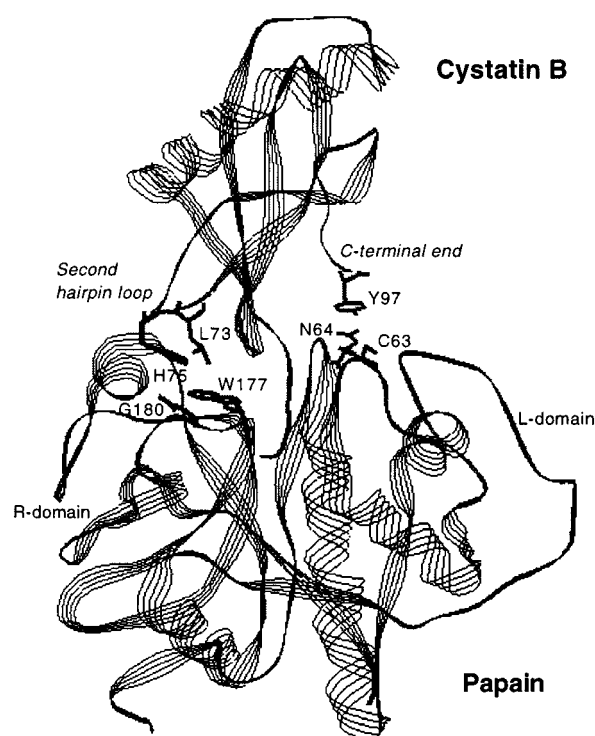


FIGURE 3: Structure of the complex of cystatin B and papain. The side chains of the amino acid residues involved in the interactions of the second hairpin loop and the C-terminal end of cystatin B with the R and L domains of papain, respectively, are shown. The figure is based on the X-ray structure determined by Stubbs et al. (19).

6–12% of the total unitary free energy of binding of the control inhibitor to these enzymes. However, the absence of an observable effect on cathepsin B binding suggests that the C-terminal end of cystatin B may be of limited importance for the interaction with this proteinase. These results are in contrast with those of a previous study, in which no effect of truncation of the C-terminal region of human cystatin B on the binding of papain was observed (27).

The decreased affinities between the cystatin B second-loop or C-terminal region mutants and those proteinases for which the kinetics could be analyzed were due almost exclusively to an increased k_{diss} , whereas k_{ass} was only slightly affected. This behavior indicates that the two regions are minimally important for the rate by which inhibitor and proteinase bind and instead contribute to the binding affinity primarily by keeping the inhibitor attached to the enzyme once the complex has been formed. In family 2 cystatins, and possibly also in cystatin A, the second binding loop is responsible for such an anchoring effect unaided by the C-terminal end of the inhibitor (20, 26, 49). However, in cystatin B the corresponding effect is exerted by a two-pronged interaction involving both the second binding loop and the C-terminal end, each binding to a different domain of the cysteine proteinase (Figure 3). The second binding loop interacts with the R domain of the proteinase, primarily the region around the highly conserved Trp-177 (papain numbering) (19). A direct hydrophobic interaction of Leu-73 with this residue is supported by the considerably reduced fluorescence change accompanying binding of the L73G/C3S variant to papain, compared to that accompanying the binding of the H75G/C3S or C3S variants. This interaction is appreciably weaker than the corresponding interaction

² The unitary free energy of binding is the free energy change after elimination of the decrease in entropy resulting from two molecules forming a complex.

made by cystatin C, which presumably involves the close stacking of the indole ring of Trp-106 in the inhibitor on that of Trp-177 in the proteinase (20, 26). However, this weaker interaction is augmented by the interaction of the neighboring His-75 with the same region of the proteinase, primarily Gly-180 adjacent to the active site cleft (19). The anchoring of the inhibitor to the target proteinase is further stabilized by interaction of Tyr-97 in the C-terminal end of cystatin B with the other proteinase domain, the L domain, mainly with Cys-63 and Asn-64. It is apparent, however, that the relative contributions of the interactions of the two regions of the inhibitor to the binding of different proteinases vary with the proteinase.

ACKNOWLEDGMENT

We are grateful to Dr. Robert W. Mason (Alfred I. duPont Institute) and Dr. I. Štern (J. Stefan Institute) for the gifts of sheep cathepsin L and bovine cathepsin B, respectively. We also thank Prof. Hans Eklund (Department of Molecular Biology, Swedish University of Agricultural Sciences) for modeling the complex of papain and bovine cystatin B and Dr. Åke Engström (Department of Medical Biochemistry and Immunology, Uppsala University, Uppsala, Sweden) for the determinations of the molecular masses of the cystatin B variants by MALDI mass spectroscopy.

REFERENCES

- Barrett, A. J., Rawlings, N. D., Davies, M. E., Machleidt, W., Salvesen, G., and Turk, V. (1986) in *Proteinase Inhibitors* (Barrett, A. J., and Salvesen, G., Eds.) pp 515–569, Elsevier, Amsterdam.
- Turk, V., and Bode, W. (1991) *FEBS Lett.* 285, 213–219.
- Abrahamson, M. (1994) *Methods Enzymol.* 244, 685–700.
- Turk, B., Turk, V., and Turk, D. (1997) *Biol. Chem. Hoppe-Seyler* 378, 141–150.
- Chapman, H. A., Riese, R. J., and Shi, G. P. (1997) *Annu. Rev. Physiol.* 59, 63–88.
- Stoka, V., Nycander, M., Lenarčič, B., Labriola, C., Cazzulo, J. J., Björk, I., and Turk, V. (1995) *FEBS Lett.* 370, 101–104.
- Korant, B., Towatari, T., Kelley, M., Brzin, J., Lenarčič, B., and Turk, V. (1988) *Biol. Chem. Hoppe-Seyler* 369 (Suppl.), 281–286.
- Collins, A. R., and Grubb, A. (1998) *Oral Microbiol. Immunol.* 13, 59–61.
- Green, G. D., Kembhavi, A. A., Davies, M. E., and Barrett, A. J. (1984) *Biochem. J.* 218, 939–946.
- Ritonja, A., Machleidt, W., and Barrett, A. J. (1985) *Biochem. Biophys. Res. Commun.* 131, 1187–1192.
- Turk, B., Križaj, I., and Turk, V. (1992) *Biol. Chem. Hoppe-Seyler* 373, 441–446.
- Ritonja, A., Coetzer, T. H. T., Pike, R. N., and Dennison, C. (1996) *Comp. Biochem. Physiol.* 114B, 193–198.
- Lenarčič, B., Križaj, I., Žunec, P., and Turk, V. (1996) *FEBS Lett.* 395, 113–118.
- Hirado, M., Iwata, D., Niinobe, M., and Fujii, S. (1981) *Biochim. Biophys. Acta* 669, 21–27.
- Pennacchio, L. A., Lehesjoki, A. E., Stone, N. E., Willour, V. L., Virtaneva, K., Miao, J. M., D'Amato, E., Ramirez, L., Faham, M., Koskinen, M., Warrington, J. A., Norio, R., De la Chapelle, A., Cox, D. R., and Myers, R. M. (1996) *Science* 271, 1731–1734.
- Pennacchio, L. A., Bouley, D. M., Higgins, K. M., Scott, M. P., Noebels, J. L., and Myers, R. M. (1998) *Nat. Genet.* 20, 251–258.
- Calkins, C. C., and Sloane, B. F. (1995) *Biol. Chem. Hoppe-Seyler* 376, 71–80.
- Šmid, L., Strojani, P., Budihna, M., Škrk, J., Vrhovec, I., Žargi, M., and Kos, J. (1997) *Eur. Arch. Otorhinolaryngol.* 254 (Suppl. 1), S150–S153.
- Stubbs, M. T., Laber, B., Bode, W., Huber, R., Jerala, R., Lenarčič, B., and Turk, V. (1990) *EMBO J.* 9, 1939–1947.
- Bode, W., Engh, R., Musil, D., Thiele, U., Huber, R., Karshikov, A., Brzin, J., Kos, J., and Turk, V. (1988) *EMBO J.* 7, 2593–2599.
- Björk, I., Alriksson, E., and Ylinenjärvi, K. (1989) *Biochemistry* 28, 1568–1573.
- Lindahl, P., Abrahamson, M., and Björk, I. (1992) *Biochem. J.* 281, 49–55.
- Machleidt, W., Thiele, U., Assfalg-Machleidt, I., Forger, D., and Auerswald, E. A. (1991) *Biomed. Biochim. Acta* 50, 613–620.
- Auerswald, E. A., Nägler, D. K., Assfalg-Machleidt, I., Stubbs, M. T., Machleidt, W., and Fritz, H. (1995) *FEBS Lett.* 361, 179–184.
- Nycander, M., and Björk, I. (1990) *Biochem. J.* 271, 281–284.
- Björk, I., Brieditis, I., Raub-Segall, E., Pol, E., Håkansson, K., and Abrahamson, M. (1996) *Biochemistry* 35, 10720–10726.
- Jerala, R., Kroon-Žitko, L., Kopitar, M., Popovič, T., and Turk, V. (1991) *Biomed. Biochim. Acta* 50, 627–629.
- Turk, B., Križaj, I., Kralj, B., Dolenc, I., Popovič, T., Bieth, J. G., and Turk, V. (1993) *J. Biol. Chem.* 268, 7323–7329.
- Leonardi, A., Turk, B., and Turk, V. (1996) *Biol. Chem. Hoppe-Seyler* 377, 319–321.
- Lindahl, P., Alriksson, E., Jörnval, H., and Björk, I. (1988) *Biochemistry* 27, 5074–5082.
- Björk, I., and Ylinenjärvi, K. (1989) *Biochem. J.* 260, 61–68.
- Björk, I., Pol, E., Raub-Segall, E., Abrahamson, M., Rowan, A. D., and Mort, J. S. (1994) *Biochem. J.* 299, 219–225.
- Mason, R. W. (1986) *Biochem. J.* 240, 285–288.
- Pol, E., Olsson, S. L., Estrada, S., Prasthofer, T. W., and Björk, I. (1995) *Biochem. J.* 311, 275–282.
- Estrada, S., Nycander, M., Hill, N. J., Craven, C. J., Waltho, J. P., and Björk, I. (1998) *Biochemistry* 37, 7551–7560.
- Jones, T. A., Zou, J.-Y., Cowan, S. W., and Kjeldgaard, M. (1991) *Acta Crystallogr.* A47, 110–119.
- Mordier, S., Béchet, D., Roux, M.-P., Obled, A., and Ferrara, M. (1993) *Biochim. Biophys. Acta* 1174, 305–311.
- Pace, C. N., Vajdos, F., Fee, L., Grimsley, G., and Gray, T. (1995) *Protein Sci.* 4, 2411–2423.
- Lenarčič, B., Ritonja, A., Šali, A., Kotnik, M., Turk, V., and Machleidt, W. (1986) in *Cysteine Proteinases and Their Inhibitors* (Turk, V., Ed.) pp 473–487, Walter de Gruyter, Berlin.
- Žerovnik, E., Jerala, R., Kroon-Žitko, L., Turk, V., and Lohner, K. (1997) *Eur. J. Biochem.* 245, 364–372.
- Jerala, R., Kroon-Žitko, L., Popovič, T., and Turk, V. (1994) *Eur. J. Biochem.* 224, 797–802.
- Musil, D., Zučič, D., Turk, D., Engh, R. A., Mayr, I., Huber, R., Popovič, T., Turk, V., Towatari, T., Katunuma, N., and Bode, W. (1991) *EMBO J.* 10, 2321–2330.
- Guncar, G., Podobnik, M., Pungertar, J., Strukelj, B., Turk, V., and Turk, D. (1998) *Structure* 6, 51–61.
- Abrahamson, M., Barrett, A. J., Salvesen, G., and Grubb, A. (1986) *J. Biol. Chem.* 261, 11282–11289.
- Popovič, T., Brzin, J., Kos, J., Lenarčič, B., Machleidt, W., Ritonja, A., Hanada, K., and Turk, V. (1988) *Biol. Chem. Hoppe-Seyler* 369 (Suppl.), 175–183.
- Nycander, M., Estrada, S., Mort, J. S., Abrahamson, M., and Björk, I. (1998) *FEBS Lett.* 422, 61–64.
- Takio, K., Kominami, E., Wakamatsu, N., Katunuma, N., and Titani, K. (1983) *Biochem. Biophys. Res. Commun.* 115, 902–908.
- Karush, F. (1962) *Adv. Immunol.* 2, 1–40.
- Martin, J. R., Craven, C. J., Jerala, R., Kroon-Žitko, L., Žerovnik, E., Turk, V., and Waltho, J. P. (1995) *J. Mol. Biol.* 246, 331–343.